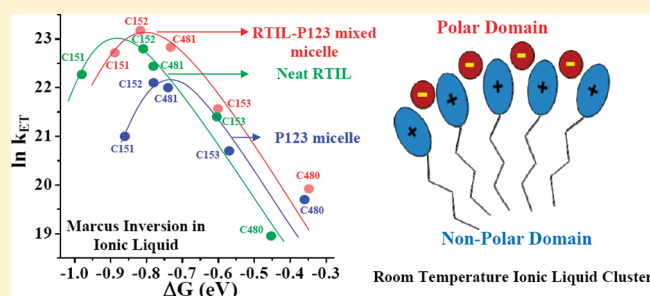


# Marcus-like Inversion in Electron Transfer in Neat Ionic Liquid and Ionic Liquid-Mixed Micelles

Atanu Kumar Das, Tridib Mondal, Supratik Sen Mojumdar, and Kankan Bhattacharyya\*

Physical Chemistry Department, Indian Association for the Cultivation of Science, Jadavpur, Kolkata 700 032, India

**ABSTRACT:** Ultrafast photoinduced electron transfer (PET) from *N,N*-dimethylaniline (DMA) to coumarin dyes in a room-temperature ionic liquid (RTIL, [pmim][BF<sub>4</sub>]) and in a mixed micelle containing the RTIL and a triblock copolymer, (PEO)<sub>20</sub>–(PPO)<sub>70</sub>–(PEO)<sub>20</sub>, (Pluronic P123) is studied using femtosecond upconversion. A Marcus-like inversion in the rate of PET is observed in neat RTIL. This is attributed to high viscosity and nanostructuring of the RTIL. Diffusion and the rate of PET in the neat RTIL are slower than those in the RTIL–P123 mixed micelle. The coumarin dyes exhibit faster electron transfer and translational diffusion (anisotropy decay) in the RTIL–P123 mixed micelle compared to that in the P123 micelle.



## 1. INTRODUCTION

Photoinduced electron transfer (PET) in a confined assembly received vigorous recent attention because of its implication in many chemical and biological processes.<sup>1–9</sup> Most recently, Lu and co-workers studied interfacial electron-transfer (ET) dynamics using a single-molecule technique.<sup>2</sup> They showed that the forward electron-transfer (FET) time exhibits a broad distribution at the single-molecule level, indicating the inhomogeneous interactions and ET reactivity of the system.<sup>2a</sup> They also studied single-molecule metal-to-ligand charge transfer dynamics using photon antibunching measurements.<sup>2b</sup> Barton and co-workers observed that DNA, when adequately coupled between the donor and acceptor, can mediate long-distance ET.<sup>3</sup> Thus, charge transfer through a DNA base pair stack gives an alternative route to carry out redox chemistry at a distance.<sup>3</sup> Sevilla and co-workers studied proton-coupled ET in DNA and found that exposure of DNA to radiation causes formation of ion radicals, which subsequently may undergo proton-coupled ET.<sup>4a</sup> Ajo-Franklin and co-workers proposed a genetic route for electron transfer across a living cell membrane, which is an insulator in nature.<sup>4b</sup> Murnane and co-workers showed that the rearrangement of the entire valence shell electron density in a molecule may be measured using a reaction microscopy technique.<sup>4c</sup> Using dark channel fluorescence yield L-edge spectroscopy, Chergui and co-workers explained the additional features shown by the fluorescence yield spectra of aqueous ionic species compared to those of nonaqueous solvents.<sup>4d</sup>

Dynamics of ET depends on solvent polarization,<sup>1</sup> vibrational modes of the solute,<sup>1</sup> and also the donor–acceptor (D–A) distance.<sup>5a</sup> In an ordinary liquid, solvation is often faster than diffusion, and the latter is rate determining in ET. In neat DMA, close proximity of the donor (solvent) and acceptor leads to a situation where ET is faster than solvation and diffusion.<sup>6</sup> Under

this condition, a Marcus-like inversion is readily observed.<sup>6</sup> In a micelle, the donor (e.g., dimethylaniline, DMA) and the acceptor stay very close to each other. This is expected to result in ultrafast ET. This expectation along with the slow solvation dynamics<sup>7</sup> makes a micelle an ideal environment to study the PET process faster than solvation dynamics. Many groups recently reported observation of Marcus-like inversion in micelles.<sup>8,9</sup>

In the present work, we focus our attention on how PET is affected in a RTIL. It is already reported that in a RTIL, the solvation dynamics display a long component of  $\sim 100$  ps.<sup>10</sup> RTILs are well-known to display persistent local structure in the nanodimension and also for its microheterogeneous nature.<sup>11,12</sup> The presence of local structure was first predicted in computer simulations.<sup>11</sup> The experimental evidence in favor of this was obtained by SAXS studies,<sup>12</sup> excitation wavelength dependence of fluorescence spectra,<sup>13</sup> and wavelength dependence of solvation dynamics.<sup>10</sup> We attempt to understand how these factors along with high viscosity of a RTIL affect PET. The slow solvation and ET in RTILs and the RTIL micelle has recently been addressed by many workers.<sup>14,15</sup> In one of the earlier works on PET in RTILs, Samanta and co-workers studied the effect of viscosity and polarity and local structure on the quenching of pyrene fluorescence by DMA.<sup>14f</sup>

We compare the results on PET in neat RTIL with that in a RTIL–copolymer mixed micelle and a copolymer micelle. It has been observed that the solvation in neat RTIL is faster than that in micelles or mixed micelles,<sup>10a</sup> and also with addition of an ionic liquid to the P123 micelle, both the solvation<sup>16a,b</sup> and ESPT<sup>16c</sup> become faster. Recently, we have studied ultrafast PET in a P123

Received: January 28, 2011

Revised: March 18, 2011

Published: April 05, 2011



RTIL–P123 mixed micelle) as

$$\nu_{\text{em}}^{\text{p}}(0) = \nu_{\text{abs}}^{\text{p}} - (\nu_{\text{abs}}^{\text{np}} - \nu_{\text{em}}^{\text{np}}) \quad (2)$$

where  $\nu_{\text{em}}^{\text{np}}$  and  $\nu_{\text{abs}}^{\text{np}}$  denote the steady-state frequencies of emission and absorption, respectively, of the probe (C480) in a nonpolar solvent (i.e., cyclohexane).<sup>18a</sup>

In the present study, we used 5 wt % P123 and 0.3 M RTIL. Using the aggregation number of  $N_{\text{agg}} \approx 155$ <sup>18b</sup> and critical micellar concentration of  $\text{CMC} \approx 0.052$  mM, the concentration of the micelle is calculated to be  $56 \mu\text{M}$ . The coumarin (electron-acceptor) concentration is  $\sim 40 \mu\text{M}$ , which is similar to that of micellar concentration.<sup>19</sup> Thus, each micelle contains approximately one acceptor molecule. The radius of the RTIL–P123 mixed micelle is reported to be  $\sim 100 \text{ \AA}$ .<sup>16b</sup> Upon addition of the highly hydrophobic RTIL [pmim][BF<sub>4</sub>], it preferentially goes to the core of the P123 micelle and remains as an ion pair. Thus, the presence of large number of the ion pairs in the core and their electrostatic repulsion may be responsible for the expansion of the core and, hence, the observed slight increase in the size in 0.3 M [pmim][BF<sub>4</sub>].<sup>16b</sup> We assumed that at a 0.3 M RTIL concentration, the corona region of P123 remains intact, and the corresponding thickness of the mixed micellar palisade layer remains the same as that of the P123 micelle ( $17 \text{ \AA}$ ).<sup>19b</sup> Thus, the volume of the mixed micellar palisade layer is  $\sim 20 \times 10^5 \text{ \AA}^3$  per mixed micelle. The local concentration of DMA  $\{[\text{DMA}]_{\text{eff}}\}$  (i.e.,  $[Q]_{\text{eff}}$ ) in the Stern (or palisade) layer of the mixed micelle was estimated as

$$[Q]_{\text{eff}} = \frac{N_{\text{ag}}[Q]}{A\{[\text{micelle}] - \text{CMC}\}} \quad (3)$$

where  $N_{\text{ag}}$  is the aggregation number of the mixed micelle ( $N_{\text{ag}} = 155$ ),<sup>18b</sup>  $[\text{micelle}]$  is the total surfactant concentration, CMC is the critical micellar concentration,  $A$  is the volume of the Stern (or palisade) layer in  $\text{dm}^3$  per mole of the micelle, and  $Q$  is the total bulk DMA concentration in molar units.

Because the available volume for the solutes inside of the micelle is restricted by the micellar wall, the effective concentration of the amine in the palisade layer of the micelle is much higher than that of the bulk concentration. Thus, an 80 mM bulk concentration of DMA corresponds to a local concentration of  $\sim 1.2$  M in the palisade layer of the P123 micelle, which is comparable with the neat DMA concentration ( $\sim 7.9$  M).

$\Delta G^0$  for a photoinduced ET reaction between an electron donor (D) and an electron acceptor (A) is given by the Rehm–Weller equation<sup>20</sup>

$$\Delta G^0 = E(\text{D}/\text{D}^+) - E(\text{C}/\text{C}^-) - E_{00} - E_{\text{IPs}} \quad (4)$$

The explanation of the terms in eq 4 and their calculations are described in our earlier works.<sup>8</sup>

The diffusion coefficient of C480 in neat RTIL is measured using the FCS technique described in our earlier works.<sup>21</sup>

### 3. RESULTS AND DISCUSSION

**3.1. Steady-State Absorption and Emission Studies in a RTIL and a RTIL–P123 Mixed Micelle.** The absorption spectra of the coumarin dyes in a neat RTIL (Figure 1) and the RTIL–P123 mixed micelle do not change significantly upon addition of DMA. This suggests that the donor (DMA) and the acceptors (coumarin) do not form any complex in the ground

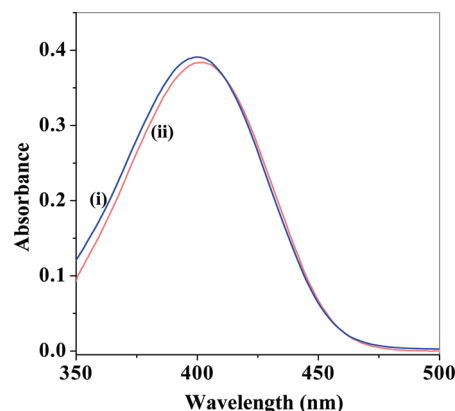


**Figure 1.** Absorption spectra of C152 in neat RTIL at bulk DMA concentrations (i) 0 (blue) and (ii) 1.5 M (red).

state and also may eliminate the possibility of static quenching. It may be mentioned that Lijun et al. observed significant change in the absorption spectra of a dye attached to  $\text{TiO}_2$ , which is ascribed to static quenching.<sup>2a</sup>

The emission maximum of the coumarin dyes in a neat RTIL and the RTIL–P123 mixed micelle exhibits a blue shift compared to that in bulk water. This indicates that both the neat RTIL and the RTIL–P123 mixed micelle are less polar than the bulk water. In the RTIL–P123 mixed micelle, coumarin dyes are located in the hydrated palisade (or Stern) layer of the mixed micelle.<sup>8</sup> The emission maxima of C151, C152, C481, C153, and C480 (Scheme 1) in a RTIL–P123 mixed micelle are found to be at 474, 486, 480, 512, and 470 nm, respectively. Comparing these with the reported<sup>22</sup> emission maxima of the coumarin dyes in different solvents, the polarity of the microenvironment of the dyes inside of a RTIL–P123 mixed micelle is estimated to be similar to that of ethanol ( $\lambda_{\text{em}} = 473 \text{ nm}$  for C480). Note, the emission maximum of C480 in the RTIL–P123 mixed micelle ( $\sim 470 \text{ nm}$ ) is red-shifted compared to that in P123 micelles ( $465 \text{ nm}$ ), while the emission maximum of the neat RTIL ( $\sim 462 \text{ nm}$ ) is almost similar to that of the P123 micelle. This indicates that the RTIL–P123 mixed micelle is more polar than P123 micelles, and the polarity of the RTIL is comparable to that of the P123 micelle.

On addition of DMA (electron donor), the emission intensity of the coumarin dyes decreases quite drastically (Figure 2). In the neat RTIL and the RTIL–P123 mixed micelle, this dramatic decrease is ascribed to ET from DMA to the coumarin dyes. It is readily seen that addition of 80 mM DMA to the mixed micelle causes a maximum decrease ( $\sim 40$  fold) in the emission intensity of C481. In the case of C480, the extent of quenching is found to be the smallest at  $\sim 3$  times in the mixed micelle (Figure 2) at a highest DMA concentration. Similar quenching was also observed for other coumarin dyes.

**3.2. Ultrafast Electron Transfer in a Neat RTIL and in a RTIL–P123 Mixed Micelle.** In both the neat RTIL and the RTIL–P123 mixed micelle, with a gradual increase in the concentration of DMA, the lifetime of coumarin dyes markedly decreases. Figures 3 and 4 reveal this phenomenon in picosecond and femtosecond transients.

In the absence of DMA, there is a rise component at a higher wavelength for all of the coumarin dyes in the neat RTIL and the mixed micelle because of solvation. No rise is observed at the red

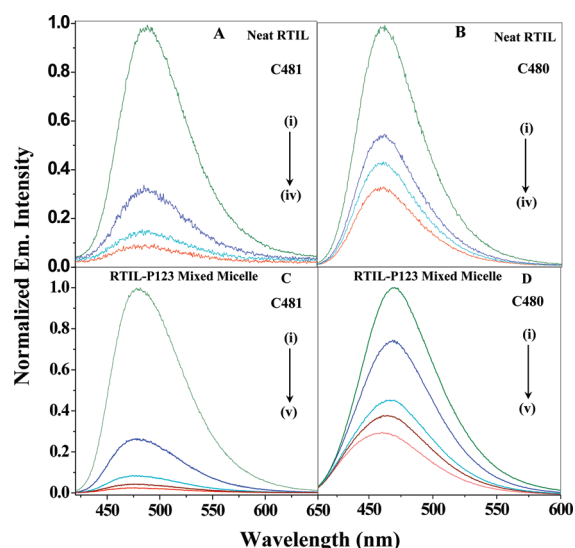


**Figure 2.** Emission spectra of C481 (A,C) and C480 (B,D) in neat RTIL (A,B) at bulk DMA concentrations (i) 0 (olive), (ii) 0.5 (blue), (iii) 1.0 (cyan), and (iv) 1.5 M (red) and in a RTIL–P123 mixed micelle (C,D) at bulk DMA concentrations (i) 0 (olive), (ii) 20 (blue), (iii) 40 (cyan), (iv) 60 (wine red), and (v) 80 mM (red) (all excitations are taken at  $\lambda_{\text{ex}} = 405$  nm).

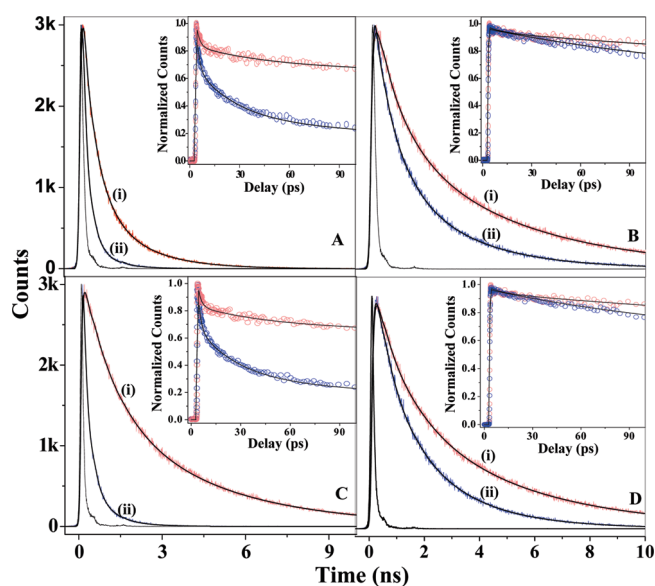


**Figure 3.** Picosecond transients ( $\lambda_{\text{ex}} = 405$  nm) of C481 (A,C at  $\lambda_{\text{em}} = 460$  nm) and C480 (B,D at  $\lambda_{\text{em}} = 440$  nm) in neat RTIL (A,B) at bulk DMA concentration (i) 0 (red) and (ii) 1.5 M (blue) and in a RTIL–P123 mixed micelle (C,D) at bulk DMA concentrations (i) 0 (red) and (ii) 80 mM (blue). Corresponding femtosecond transients are shown in the insets.

end of the decay of the coumarin dyes in the presence of DMA (except C480) (Table 1). The absence of a rise component at the red end indicates that ET is faster than the solvation. Thus, the rise is masked by ultrafast decay of the quenched emission of all of the coumarin dyes except C480 in the mixed micelle. In contrast to these four coumarin dyes, the extent of quenching for C480 is very small, and it shows a rise at the red end even at very high DMA concentration.

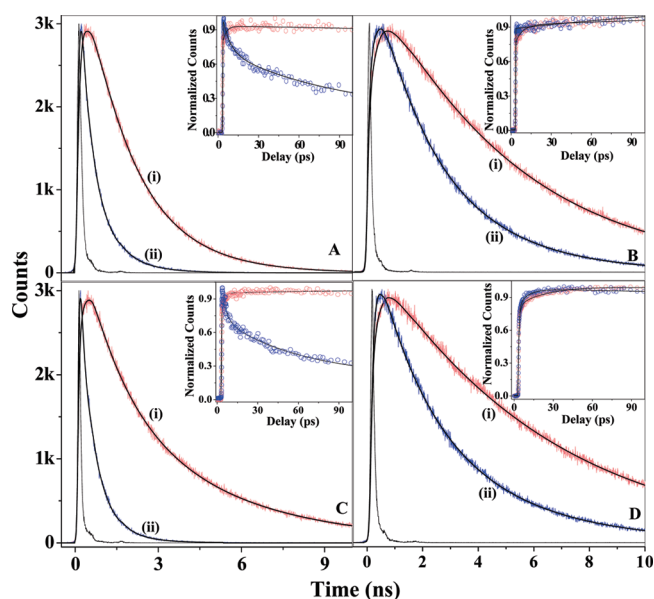


**Figure 4.** Picosecond transients ( $\lambda_{\text{ex}} = 405$  nm) of C481 (A,C) at  $\lambda_{\text{em}} = 540$  nm and C480 (B,D) at  $\lambda_{\text{em}} = 500$  nm in neat RTIL (A,B) at bulk DMA concentrations (i) 0 (red) and (ii) 1.5 M (blue) and in a RTIL–P123 mixed micelle (C,D) at bulk DMA concentrations (i) 0 (red) and (ii) 80 mM (blue). Corresponding femtosecond transients are shown in the insets.

**Table 1.** Fluorescence Decay Parameters of Coumarin Dyes in a Neat RTIL at 0 and 1.5 M Bulk DMA Concentration

acceptor	$\lambda_{\text{em}}$ (nm)	[DMA] (M)	$\tau_1$ ( $a_1$ ) <sup>a</sup> (ps)	$\tau_2$ ( $a_2$ ) <sup>a</sup> (ps)	$\tau_3$ ( $a_3$ ) <sup>a</sup> (ps)
C151	440	0	3.5 (0.01)	280 (0.02)	3875 (0.97)
		1.5	2 (0.5)	18 (0.33)	740 (0.17)
	540	0	1.5 (−0.13)	100 (−0.24)	5600 (1.37)
		1.5	1.5 (0.79)	29 (0.12)	1685 (0.09)
C152	460	0	6.5 (0.12)	97 (0.25)	1075 (0.63)
		1.5	1 (0.57)	19 (0.27)	417 (0.16)
	540	0	2 (−0.26)	321 (−1.17)	2100 (2.43)
		1.5	3 (0.35)	48 (0.38)	1080 (0.27)
C481	460	0	4 (0.1)	82 (0.18)	940 (0.72)
		1.5	1 (0.4)	21 (0.38)	440 (0.22)
	540	0	2.5 (−0.19)	380 (−0.31)	1800 (1.5)
		1.5	5.5 (0.28)	81 (0.49)	740 (0.23)
C153	490	0	3.5 (0.12)	100 (0.45)	2720 (0.43)
		1.5	2.5 (0.25)	21 (0.33)	680 (0.42)
	550	0	2 (−0.18)	335 (−0.01)	5500 (1.19)
		1.5	1.5 (0.05)	110 (0.6)	1900 (0.35)
C480	440	0	4.5 (0.01)	110 (0.01)	3080 (0.98)
		1.5	6.5 (0.02)	90 (0.05)	1650 (0.93)
	500	0	5.5 (−0.19)	1670 (−2.11)	4950 (3.3)
		1.5	4.5 (−0.05)	275 (−0.5)	2500 (1.55)

<sup>a</sup> Error:  $\pm 10\%$ .

In order to determine the rate constant of the ET process ( $k_{\text{ET}}$ ), we used the equation<sup>8</sup>

$$\frac{1}{\tau} = \frac{1}{\tau_0} + k_{\text{ET}}[Q]_{\text{eff}} \quad (5)$$

where  $\tau$  and  $\tau_0$  denote the lifetime of the acceptor (coumarin) in the presence and in the absence of the quencher Q (DMA).  $[Q]_{\text{eff}}$  denotes the local or effective concentration of the quencher in the Stern layer of the micelle or mixed micelle. In the absence of the amine, the faster components of decay at the blue end are due



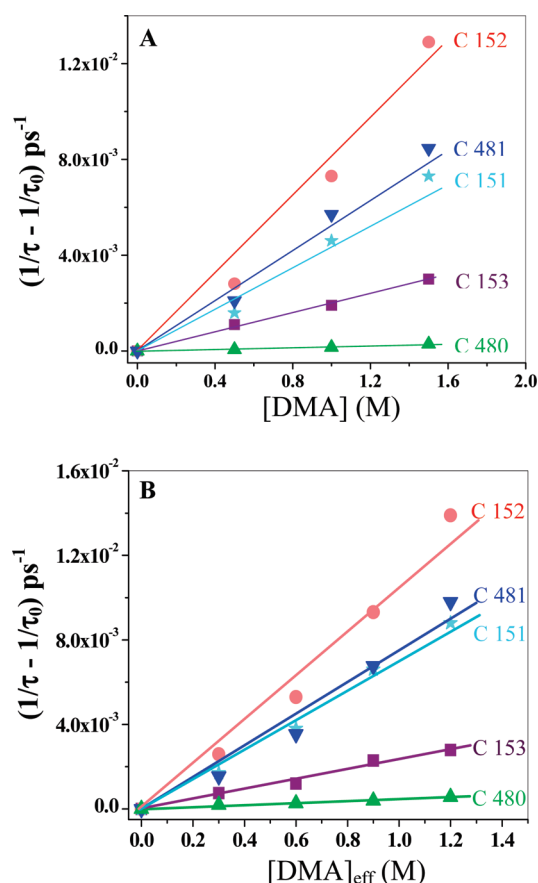


**Figure 5.** Stern–Volmer plots for C152 (red), C481 (blue), C151 (cyan), C153 (purple), and C480 (green) in neat RTIL (A) and a RTIL–P123 mixed micelle (B) at different local DMA concentrations.

to solvation dynamics for all of the coumarin dyes. Therefore, we used the slow component of the decay at the blue end as  $\tau_0$ .

In the neat RTIL, the bulk DMA concentration is considered. In the presence of DMA, we used the average lifetime of the fluorescence decays of C151, C152, C481, and C153 (at blue end,  $\lambda_{\text{em}} \approx 460$  nm) as  $\tau$ . The fluorescence decays of the coumarin dyes at the blue end are multiexponential because of solvation dynamics. Note that ET also involves a multiple-time scale.<sup>1c,d</sup> At short time scale, both ET and solvation dynamics compete. This may cause a slight deviation of the curves in Figure 5 from linearity. For C480, because solvation is faster than ET (indicated by the rise component at the red end even at high DMA concentration (Figure 4B)), we used the slow component of decay at the blue end as  $\tau$  at all amine concentrations.

The rate constants of PET are determined from the Stern–Volmer plots (Figure 5A) and are different for different dyes in the neat RTIL (Table 2). In the neat RTIL, C152 shows the fastest ET rate ( $\sim 80.0 \times 10^8 \text{ M}^{-1} \text{ s}^{-1}$ ), and C480 exhibits the slowest ET rate ( $1.7 \times 10^8 \text{ M}^{-1} \text{ s}^{-1}$ ). Thus, in the neat RTIL, C152 exhibits  $\sim 50$  times faster ET compared to that of C480.

In the mixed micelle, at an 80 mM bulk DMA concentration, C480 exhibits an ultrafast rise component of  $\sim 3$  ps (Figure 4D and Table 3), which roughly equals the ultrafast component of solvation. For the mixed micelle, we used  $[Q]_{\text{eff}}$  (eq 3). The values of  $\tau$  and  $\tau_0$  were determined similarly as in the case of the neat RTIL. The rate constants of ET for the mixed micelle (obtained from Figure 5B) are listed in Table 4. In the mixed

**Table 2.** Electron-Transfer Parameters of Coumarin Dyes in a Neat RTIL at Different DMA Concentrations

probe	[DMA] M	$\Delta G^0$ (eV)	$\langle \tau \rangle^{a,b}$ (ps)	$k_{\text{ET}}$ ( $\text{s}^{-1} \text{ M}^{-1}$ )	$\ln(k_{\text{ET}})$
C151	0		3875 <sup>c</sup>		
	0.5	−0.98	1785 <sup>a</sup>	$47.0 \times 10^8$	22.3
	1.0		950 <sup>a</sup>		
	1.5		745 <sup>a</sup>		
C152	0		1075 <sup>c</sup>		
	0.5	−0.81	265 <sup>a</sup>	$80.1 \times 10^8$	22.8
	1.0		120 <sup>a</sup>		
	1.5		72 <sup>a</sup>		
C481	0		940 <sup>c</sup>		
	0.5	−0.78	320 <sup>a</sup>	$55.5 \times 10^8$	22.4
	1.0		150 <sup>a</sup>		
	1.5		105 <sup>a</sup>		
C153	0		2720 <sup>c</sup>		
	0.5	−0.60	680 <sup>a</sup>	$19.8 \times 10^8$	21.4
	1.0		440 <sup>a</sup>		
	1.5		295 <sup>a</sup>		
C480	0	−0.45	3080 <sup>c</sup>	$1.7 \times 10^8$	19.0
	0.5		2630 <sup>c</sup>		
	1.0		2100 <sup>c</sup>		
	1.5		1645 <sup>c</sup>		

<sup>a</sup>  $\langle \tau \rangle = \sum a_i \tau_i$ . <sup>b</sup> Error:  $\pm 10\%$ . <sup>c</sup> Longest component of decay.

**Table 3.** Fluorescence Decay Parameters of Coumarin Dyes in a 0.3 M RTIL–P123 (5 wt %) Mixed Micelle at 0 and 80 mM Bulk DMA Concentration

acceptor	$\lambda_{\text{em}}$ (nm)	[DMA] (mM)	$\tau_1$ ( $a_1$ ) <sup>a</sup> (ps)	$\tau_2$ ( $a_2$ ) <sup>a</sup> (ps)	$\tau_3$ ( $a_3$ ) <sup>a</sup> (ps)
C151	440	0	2.5 (0.26)	250 (0.46)	3600 (0.28)
		80	1 (0.49)	30 (0.3)	480 (0.21)
		540	0	3.5 (−0.32)	365 (−0.1)
C152	460	0	3.5 (0.20)	64 (0.4)	3300 (0.4)
		80	7.5 (0.23)	275 (0.31)	2570 (0.46)
		540	0	1.5 (−0.25)	180 (−0.01)
C481	460	0	2 (0.28)	42 (0.44)	900 (0.282)
		80	3.5 (0.21)	350 (0.35)	2650 (0.44)
		540	0	3 (0.43)	50 (0.35)
C153	490	0	2 (−0.25)	270 (−0.23)	3260 (1.48)
		80	3.5 (0.28)	60 (0.49)	840 (0.23)
		550	0	19 (0.05)	370 (0.64)
C480	440	0	4.5 (0.16)	70 (0.47)	4000 (0.31)
		80	3 (−0.10)	2250 (−2.5)	5500 (3.6)
		500	0	8.5 (0.05)	150 (0.5)
	500	0	4.5 (0.12)	350 (0.08)	3150 (0.8)
		80	9 (0.01)	200 (0.37)	1700 (0.62)
		80	6.5 (−0.3)	2850 (−3.6)	5700 (4.9)
	80	0	3 (−0.42)	1750 (0.17)	3650 (1.25)

<sup>a</sup> Error:  $\pm 10\%$ .

micelle, C152 exhibits the fastest ET ( $\sim 116 \times 10^8 \text{ M}^{-1} \text{ s}^{-1}$ ), while C480 shows the slowest ET ( $\sim 4.7 \times 10^8 \text{ M}^{-1} \text{ s}^{-1}$ ). Thus, in the mixed micellar system, C152 shows  $\sim 20$  fold faster ET compared to that of C480.

It may be noted that the rate of ET (for C152) in the neat RTIL ( $80.0 \times 10^8 \text{ M}^{-1} \text{ s}^{-1}$ ) is  $\sim 1.5$  times slower compared to that in the RTIL–P123 mixed micelle. This may be ascribed to the higher viscosity and lower polarity of the neat RTIL.

**3.3. Solvation Dynamics in the Presence of DMA.** Addition of DMA to the RTIL and RTIL mixed micelle does not affect solvation dynamics to a large extent. Figure 6A shows the TRES, and Figure 6B exhibits the decay of the solvent correlation function,  $C(t)$ , for C480 in the RTIL–P123 mixed micelle in

**Table 4. Electron-Transfer Parameters of Coumarin Dyes in a RTIL (0.3 M)–5 wt % P123 Mixed Micelle at Different DMA Concentrations**

probe	[DMA] mM	[DMA] <sub>eff</sub> <sup>a</sup> (M)	$\Delta G^0$ (eV)	$\langle\tau\rangle^{b,c}$ (ps)	$k_{ET}$ (s <sup>-1</sup> M <sup>-1</sup> )	ln( $k_{ET}$ )
C151	0	—	−0.89	3600 <sup>d</sup>	$73.4 \times 10^8$	22.7
	20	0.3		500 <sup>b</sup>		
	40	0.6		245 <sup>b</sup>		
	60	0.9		145 <sup>b</sup>		
	80	1.2		110 <sup>b</sup>		
C152	0	—	−0.82	2570 <sup>d</sup>	$115.8 \times 10^8$	23.2
	20	0.3		340 <sup>b</sup>		
	40	0.6		176 <sup>b</sup>		
	60	0.9		103 <sup>b</sup>		
	80	1.2		70 <sup>b</sup>		
C481	0	—	−0.73	2650 <sup>d</sup>	$89.5 \times 10^8$	22.9
	20	0.3		524 <sup>b</sup>		
	40	0.6		255 <sup>b</sup>		
	60	0.9		140 <sup>b</sup>		
	80	1.2		98 <sup>b</sup>		
C153	0	—	−0.60	4000 <sup>d</sup>	$23.2 \times 10^8$	21.6
	20	0.3		990 <sup>b</sup>		
	40	0.6		690 <sup>b</sup>		
	60	0.9		390 <sup>b</sup>		
	80	1.2		330 <sup>b</sup>		
C480	0	—	−0.35	3150 <sup>d</sup>	$4.7 \times 10^8$	20.0
	20	0.3		1975 <sup>c</sup>		
	40	0.6		1710 <sup>c</sup>		
	60	0.9		1400 <sup>c</sup>		
	80	1.2		1130 <sup>c</sup>		

<sup>a</sup> [DMA]<sub>eff</sub> denotes the local concentration of DMA in the palisade layer of the RTIL–P123 mixed micelle. <sup>b</sup>  $\langle\tau\rangle = \sum a_i \tau_i$ . <sup>c</sup> Error:  $\pm 10\%$ . <sup>d</sup> Longest component of decay. <sup>e</sup>  $\langle\tau\rangle = (a_1 \tau_1 + a_2 \tau_2)$ , average of the two longest components.

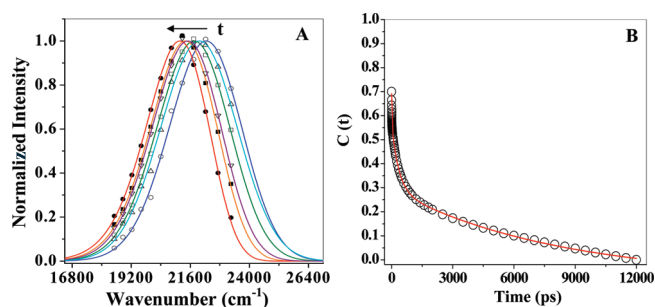


**Figure 6.** (A) Time-resolved emission spectra (TRES) of C480 in the presence of 20 mM DMA in a RTIL–P123 mixed micelle at 0 (○, blue), 50 (△, cyan), 300 (□, olive), 1500 (▽, purple), 3000 (■, orange), and 10000 ps (●, red). (B) Solvent response function  $C(t)$  of C480 in the presence of 20 mM DMA in a RTIL–P123 mixed micelle.

the presence of 20 mM DMA. The components of solvation dynamics are found to be 5 (13%), 350 (27%), and 4000 ps (30%) (Table 5). It is observed that about 30% of the solvation dynamics is faster than the IRF ( $\sim 350$  fs) of our femtosecond setup. This suggests that there is a component ( $\sim 43\%$ ) of solvation that is on a time scale of  $\leq 10$  ps. The ultrafast component of solvation obviously facilitates the ultrafast component of ET, which occurs on a  $\sim 10$  ps time scale. It is observed that the ET process in the mixed micellar system is  $\sim 3$  times faster than that for the P123 micelle reported earlier.<sup>8d</sup> Thus, it is interesting to note that with the addition of a RTIL (0.3 M) to the P123 micelle, the ET process becomes  $\sim 3$ -fold faster. The faster

ET in a mixed micelle compared to that for the P123 micelle may be attributed to the faster solvation in the RTIL–P123 mixed micelle (major component 4000 ps;  $\tau_{av.} \approx 1300$  ps) compared to that in the P123 micelle (major component 4500 ps;  $\tau_{av.} = 2600$  ps)<sup>8d</sup> and the higher polarity of the RTIL–P123 system.

Previously, we studied solvation dynamics of C480 in the neat RTIL.<sup>10a</sup> It is observed that the solvation dynamics in the neat RTIL (major component = 2200 ps;  $\tau_{av.} \approx 680$  ps) is  $\sim 2$  times faster compared to that in the RTIL–P123 mixed micelle. In this case, the slower ET rate in the neat RTIL may be rationalized by a higher viscosity and slower diffusion compared to that in the RTIL–P123 mixed micelle.

**3.4. Anisotropy Decay in the RTIL and RTIL–P123 Mixed Micelle.** The anisotropy decay parameters of different dyes in the neat RTIL and RTIL–P123 mixed micelle are shown in Table 6. The anisotropy decay of C480 in the neat RTIL (at  $\lambda_{ex} = 405$  nm) is single-exponential with a time constant of 3800 ps<sup>10a</sup> and is much slower than that of bulk water (70 ps).<sup>10a</sup> The slower anisotropy in the neat RTIL may be attributed to the higher viscosity of the RTIL ( $\sim 135$  cP).<sup>21</sup> The anisotropy decay in both the P123 micelle and the mixed micelle is found to be slower compared to that in bulk water and is biexponential

$$r(t) = r_0 [\beta \exp(-t/\tau_{slow}) + (1 - \beta) \exp(-t/\tau_{fast})]$$

The RTIL–P123 mixed micelle at  $\lambda_{ex} = 405$  nm for C480 shows two components of anisotropy decay, 400 (35%) and 2500 ps (65%), with  $\langle\tau_{rot}\rangle = 1750$  ps.<sup>16b</sup> Experimental studies reveal that the average rotational time of C480 in the neat RTIL (3800 ps)<sup>10a</sup> is  $\sim 1.3$  times and  $\sim 2.2$  times slower compared to that in the P123 micelle (3000 ps)<sup>16b</sup> and the RTIL–P123 mixed micelle (1750 ps),<sup>16b</sup> respectively. The faster rotation in the RTIL–P123 mixed micelle compared to that in the P123 micelle may be ascribed to the disentanglement of the P123 chains by the RTILs. In the RTIL–P123 mixed micelle, the ion pairs become separated by polymer chains. Thus, the friction in the RTIL–P123 mixed micelle is less than that in the neat RTIL.

**3.5. Diffusion in the Neat RTIL and RTIL–P123 Mixed Micelle.** The diffusion constant ( $D_t$ ) of C480 in the neat RTIL is measured using the FCS technique and is found to be  $7.0 \times 10^{-12}$  m<sup>2</sup> s<sup>-1</sup>.<sup>21c</sup> Evidently, the diffusion constant of C480 in the neat RTIL is  $\sim 100$  times slower than that in bulk water ( $D_t \approx 6.0 \times 10^{-10}$  m<sup>2</sup> s<sup>-1</sup>).<sup>21a</sup> The slower diffusion in the neat RTIL may be due to the higher viscosity ( $\sim 135$  cP),<sup>23</sup> which is nearly 135 times higher than that of water ( $\sim 1$  cP).

In the micelles, the  $D_t$  values are calculated using the wobbling-in-cone model.<sup>24</sup> In the RTIL–P123 mixed micelle, the  $D_t$  of C480 is found to be  $7.0 \times 10^{-9}$  m<sup>2</sup> s<sup>-1</sup>. The  $D_t$  of C480 in the mixed micelle is  $\sim 1000$  times faster than that in the neat RTIL due to the lower viscosity and higher polarity of the RTIL–P123 mixed micelle compared to that of the neat RTIL. The diffusion constant of C480 in the P123 micelle is found to be  $D_t = 2.0 \times 10^{-9}$  m<sup>2</sup> s<sup>-1</sup> for C480.<sup>25</sup> Due to the lower viscosity and higher polarity, the coumarin dyes show faster diffusion in the RTIL–P123 mixed micelle than that in the P123 micelle.

As discussed by Murata and Tachiya,<sup>5a</sup> ET needs coincidence of free energy and hence is restricted to those donor–acceptor pairs that undergoes diffusion prior to ET to achieve coincidence of energy.<sup>5a</sup> Several groups have considered this aspect in the role of diffusion on PET.<sup>5b,c</sup> The diffusion distance ( $(2D_t\tau)^{1/2}$ ) of coumarin dyes was calculated in the neat RTIL and along the micellar surface by using the  $D_t$  value in the neat RTIL ( $D_t \approx 7.0 \times 10^{-12}$  m<sup>2</sup> s<sup>-1</sup>), the

**Table 5.** Decay Parameters of  $C(t)$  of C480 in the RTIL (0.3 M)–P123 (5 wt %) Mixed Micelle, the P123 Micelle, and the Neat RTIL

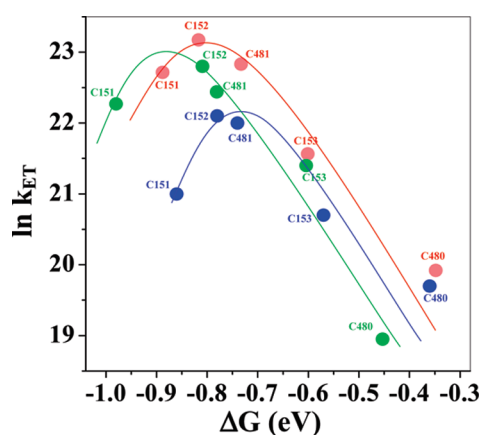
system	[DMA], bulk	total solvent shift detected, $\Delta\nu$ (cm <sup>-1</sup> )	$\tau_1^a$ ( $a_1$ ) (ps)	$\tau_2^a$ ( $a_2$ ) (ps)	$\tau_3^a$ ( $a_3$ ) (ps)	$\tau_4^a$ ( $a_4$ ) (ps)	$\tau_{ET}^{C481}$ ( $=1/k_{ET}^{C481}$ ) (ps) <sup>b</sup>
RTIL–P123 mixed micelle	20 mM	1120	$\leq 0.3$ (30%)	5 (13%)	350 (27%)	4000 (30%)	110
P123 micelle	5 mM <sup>c</sup>	1450 <sup>c</sup>	$\leq 0.3^c$ (13%)	10 <sup>c</sup> (16%)	750 <sup>c</sup> (16%)	4500 <sup>c</sup> (55%)	280
neat RTIL	0 M	625 <sup>d</sup>	$\leq 0.3^d$ (42%)	2 <sup>d</sup> (3%)	250 <sup>d</sup> (26%)	2200 <sup>d</sup> (28%)	180

<sup>a</sup>Error:  $\pm 10\%$ . <sup>b</sup>Electron-transfer time for C481 ( $\tau_{ET}^{C481}$ ) in the RTIL–P123 mixed micelle and P123 micelle. <sup>c</sup>From ref 25. <sup>d</sup>From ref 10a.

**Table 6.** Anisotropy Decay Parameters and Diffusion Constants of C480 in the (0.3 M) RTIL–P123 (5 wt %) Mixed Micelle, the P123 Micelle, and the Neat RTIL

system	$r_0$	$\tau_{r1}^a$ ( $b_1$ ) (ps)	$\tau_{r2}^a$ ( $b_2$ ) (ps)	$\langle\tau_{rot}\rangle$ (ps)	diffusion constant ( $D_t$ ) m <sup>2</sup> s <sup>-1</sup>
0.3 M RTIL + 5 wt % P123	0.35	400 (0.35)	2500 (0.65)	1750	$7.0 \times 10^{-9}$
P123 micelle	0.34	670 (0.22)	3700 (0.78)	3000	$2.0 \times 10^{-9}$
neat RTIL	0.35	3800 (1.00)		3800	$7.0 \times 10^{-12}$

<sup>a</sup>Error:  $\pm 10\%$ .

**Figure 7.** Plot of  $\ln(k_{ET})$  versus  $-\Delta G^0$  for the coumarin–DMA system in (i) a neat RTIL (green), (ii) a RTIL–P123 mixed micelle (red), and (iii) the P123 micelle (blue).

RTIL–P123 mixed micelle ( $D_t = 7.0 \times 10^{-9}$  m<sup>2</sup> s<sup>-1</sup>), and the P123 micelle ( $D_t = 2.00 \times 10^{-9}$  m<sup>2</sup> s<sup>-1</sup>)<sup>23</sup> within the average time  $\langle\tau_{ET}\rangle$  of ET. The magnitudes of these distances are 1.5, 28, and 20 Å in the neat RTIL, mixed micelle, and P123 micelle, respectively. Diffusion over such a small distance seems to be necessary to achieve coincidence of free energy for ET to occur.

It may be recalled that our previous PET study in the P123 micelle showed that PET does not depend on  $\lambda_{ex}$ .<sup>8d</sup> This is because of diffusion of donors or acceptors prior to ET obscures detection of the effect of heterogeneity in the micelle.

**3.6.  $\Delta G$  Dependence of PET in the Neat RTIL and RTIL–P123 Mixed Micelle.** Figure 7 describes the  $\Delta G$  dependence of PET in the neat RTIL and RTIL–P123 mixed micelle. The Rehm–Weller equation (eq 4) is used to calculate the free-energy change ( $\Delta G$ ) of the PET in the neat RTIL and RTIL–P123 mixed micelle.<sup>20</sup> The calculated  $\Delta G$  values are listed in Tables 2 and 4. The  $\Delta G$ -dependent rate constants of PET for the five coumarin dyes in the neat RTIL, RTIL–P123 mixed micelle, and P123 micelle are shown in Figure 7. Figure 7 clearly exhibits a bell-shaped dependence of PET on  $\Delta G$  and, thus, Marcus-type inversion. It should be further noted that the shapes of the curves in Figure 7 are asymmetric. The asymmetry may be ascribed to the inverted regime where ET becomes irreversible.

The observation of Marcus inversion in the neat RTIL is particularly interesting because such inversion is rarely observed in bulk liquid (except in neat DMA<sup>6</sup>). The unique feature of Marcus inversion in a bulk RTIL may be due to the high viscosity of the neat RTIL ( $\sim 135$  cP).<sup>23</sup> Diffusion in the neat RTIL is very slow because of the very high viscosity of the RTIL. The other cause of Marcus inversion in the neat RTIL may be the nanostructural organization and presence of clearly demarcated polar and nonpolar domains in the neat RTIL. Because of the nanoscale organization, the donor and acceptor species remain in close proximity, resulting in ET faster than the solvation in the neat RTIL.

It may be noted that the inversion occurs at different  $\Delta G$  values in the neat RTIL, RTIL–P123 mixed micelle, and P123 micelle. We will try to rationalize this. In the present work, the ET corresponds to a situation where solvation is incomplete, that is, the solvent is nonequilibrated. In such conditions, many groups have used a 2D-ET model.<sup>1c,d,6c,8,20</sup> In this model, the free energy of activation depends on the solvent coordinate ( $X$ ) as<sup>6f,26</sup>

$$k(X) = \frac{2\pi}{\hbar} V_{el}^2 (4\pi\lambda_1 k_B T)^{-1/2} \exp\left(\frac{-\Delta G^*(X)}{k_B T}\right) \quad (6)$$

$\Delta G^*$  is the free energy of activation, and  $\lambda_1$  is the intramolecular reorganization energy. In the case of ET faster than solvation, the effective solvent reorganization energy,  $\lambda_{eff}$  is less than  $\lambda_s$  when solvation is complete.  $\lambda_{eff}$  is related to  $\lambda_s$  as<sup>6c,f,26</sup>

$$\lambda_{eff} = \lambda_s (1 - 2X_g^2) \quad (7)$$

where  $X_g$  denotes nonequilibrated solvation coordinate. For the coumarin dye–DMA system,  $\lambda_s \approx 0.93$  eV and  $\lambda_1 = 0.3$  eV.<sup>5c,8b</sup>

In order to estimate the amount of reorganization energy lost ( $2\lambda_s X_g^2$ ) because of incomplete solvation, we studied solvation dynamics of C480 in the neat RTIL<sup>10a</sup> and in the mixed micelle in the presence of 20 mM DMA. Figure 6B shows the decay of the solvent correlation function  $C(t)$ , and Table 5 summarizes the parameters of the decay of  $C(t)$ , that is, the solvation dynamics in the mixed micelle. Comparing the time constant of ET near the inversion point and solvation dynamics (Table 5) in the mixed micelle, we observed that only  $\sim 45\%$  (for the neat RTIL) and  $\sim 43\%$  (for the mixed micelle) of solvation is found to be complete within



ET time. Therefore, for the neat RTIL,  $\lambda_{\text{eff}} \approx 0.45 \times \lambda_s = 0.42$  eV, and for the RTIL–P123 mixed micelle,  $\lambda_{\text{eff}} \approx 0.43 \times \lambda_s = 0.4$  eV. Thus, for the neat RTIL and RTIL–P123 mixed micelle, one should observe Marcus inversion at  $-\Delta G^0 = \lambda_{\text{eff}} + \lambda_1 \approx 0.72$  and 0.7 eV, respectively. This is close to the observed inversion at  $\sim 0.85$  (for the neat RTIL) and  $\sim 0.8$  eV (for the mixed micelle) (Figure 7). This shows that the  $\sim 45\%$  of ultrafast solvation is enough to bring about Marcus inversion in the neat RTIL and RTIL–P123 mixed micelle.

In summary, the different inversion points at different  $\Delta G$  values arise from difference in the reorganization energy in the three systems. As the reorganization energy in the neat RTIL is lower than that of the RTIL–P123 mixed micelle, the point of inversion appears at a lower  $\Delta G$  value.

#### 4. CONCLUSIONS

The main finding of this work may be summarized as follows. The most important observation is the occurrence of Marcus-like inversion in the neat RTIL and RTIL–P123 mixed micelle. The position of the inversion appears at different  $\Delta G$  values due to the difference in the reorganization energy. Diffusion plays a very crucial role in PET. The occurrence of Marcus-like inversion in the neat RTIL is ascribed to the high viscosity of the RTIL. The high viscosity and nanoscale organization keep the donor and acceptor at close proximity for enough time for ET to occur.

#### AUTHOR INFORMATION

##### Corresponding Author

\*E-mail: pckb@iacs.res.in. Fax: +91-33-2473-2805.

#### ACKNOWLEDGMENT

Thanks are due to the Department of Science and Technology, India (Center for Ultrafast Spectroscopy and Microscopy, J. C. Bose Fellowship), and the Council of Scientific and Industrial Research (CSIR) for generous research grants. A.K.D., T.M., and S.M. thank CSIR for awarding fellowships.

#### REFERENCES

- (a) Marcus, R. A. *Adv. Chem. Phys.* **1999**, 106, 1. (b) Sumi, H.; Marcus, R. A. *J. Chem. Phys.* **1986**, 84, 4894. (c) Bagchi, B.; Gayathri, N. *Adv. Chem. Phys.* **1999**, 107, 1. (d) Gayathri, N.; Bagchi, B. *J. Phys. Chem.* **1996**, 100, 3056. (e) Tachiya, M. *J. Phys. Chem.* **1993**, 97, 5411. (f) Roy, S.; Bagchi, B. *J. Phys. Chem.* **1994**, 98, 9207.
- (a) Lijun, G.; Yuanmin, W.; Lu, H. P. *J. Am. Chem. Soc.* **2010**, 132, 1999. (b) Hu, D.; Lu, H. P. *J. Phys. Chem. B* **2005**, 109, 9861. (c) Wang, Y.; Wang, X.; Ghosh, S. K.; Lu, H. P. *J. Am. Chem. Soc.* **2009**, 131, 1479. (d) Biju, V.; Micic, M.; Hu, D.; Lu, H. P. *J. Am. Chem. Soc.* **2004**, 126, 9374.
- (a) Genereux, J. C.; Barton, J. K. *Chem. Rev.* **2010**, 110, 1642. (b) Genereux, J. C.; Boal, A. K.; Barton, J. K. *J. Am. Chem. Soc.* **2010**, 132, 891. (c) Tanaka, M.; Elias, B.; Barton, J. K. *J. Org. Chem.* **2010**, 75, 2423.
- (a) Kumar, A.; Sevilla, M. D. *Chem. Rev.* **2010**, 110, 7002. (b) Jensen, H. M.; Albers, A. E.; Malley, K. R.; Londer, Y. Y.; Cohen, B. E.; Helms, B. A.; Weigele, P.; Groves, J. T.; Ajo-Franklin, C. M. *Proc. Natl. Acad. Sci. U.S.A.* **2010**, 107, 19213. (c) Li, W.; Jaroń-Becker, A. A.; Hogle, C. W.; Sharma, V.; Zhou, X.; Becker, A.; Kapteyn, H. C.; Murnane, M. M. *Proc. Natl. Acad. Sci. U.S.A.* **2010**, 107, 20219. (d) Aziz, E. F.; Rittmann-Frank, M. H.; Lange, K. M.; Bonhommeau, S.; Chergui, M. *Nat. Chem.* **2010**, 2, 853.
- (a) Murata, S.; Tachiya, M. *J. Phys. Chem. A* **2007**, 111, 9240. (b) Saik, V. O.; Goun, A. A.; Nanda, J.; Shirota, K.; Tavernier, H. L.; Fayer, M. D. *J. Phys. Chem. A* **2004**, 108, 6696. (c) Tavernier, H. L.; Laine, F.; Fayer, M. D. *J. Phys. Chem. A* **2001**, 105, 8944.
- (a) Yoshihara, K. *Adv. Chem. Phys.* **1999**, 107, 371. (b) Kobayashi, T.; Takagi, Y.; Kandori, H.; Kemnitz, K.; Yoshihara, K. *Chem. Phys. Lett.* **1991**, 180, 416. (c) Pal, H.; Nagasawa, Y.; Tominaga, K.; Yoshihara, K. *J. Phys. Chem.* **1996**, 100, 11964. (d) Shirota, H.; Pal, H.; Tominaga, K.; Yoshihara, K. *J. Phys. Chem. A* **1998**, 102, 3089. (e) Shirota, H.; Pal, H.; Tominaga, K.; Yoshihara, K. *Chem. Phys.* **1998**, 236, 355. (f) Yoshihara, K.; Tominaga, K.; Nagasawa, Y. *Bull. Chem. Soc. Jpn.* **1995**, 68, 696.
- (a) Nandi, N.; Bhattacharyya, K.; Bagchi, B. *Chem. Rev.* **2000**, 100, 2013. (b) Riter, R. E.; Willard, D. M.; Levinger, N. E. *J. Phys. Chem. B* **1998**, 102, 2705. (c) Piletic, I. R.; Moilanen, D. E.; Spry, D. B.; Levinger, N. E.; Fayer, M. D. *J. Phys. Chem. B* **2006**, 110, 4985. (d) Senapati, S.; Chandra, A. *J. Phys. Chem. B* **2001**, 105, 5106.
- (a) Ghosh, S.; Sahu, K.; Mondal, S. K.; Sen, P.; Bhattacharyya, K. *J. Chem. Phys.* **2006**, 125, 054509. (b) Ghosh, S.; Mondal, S. K.; Sahu, K.; Bhattacharyya, K. *J. Chem. Phys.* **2007**, 126, 204708. (c) Ghosh, S.; Mondal, S. K.; Sahu, K.; Bhattacharyya, K. *J. Phys. Chem. A* **2006**, 110, 13139. (d) Mandal, U.; Ghosh, S.; Dey, S.; Adhikari, A.; Bhattacharyya, K. *J. Chem. Phys.* **2008**, 128, 164504. (e) Ghosh, S.; Mandal, U.; Adhikari, A.; Dey, S.; Bhattacharyya, K. *Int. Rev. Phys. Chem.* **2007**, 26, 421.
- (a) Kumbhakar, M.; Nath, S.; Mukherjee, T.; Pal, H. *J. Chem. Phys.* **2004**, 120, 2824. (b) Kumbhakar, M.; Singh, P. K.; Satpati, S. K.; Nath, S.; Pal, H. *J. Phys. Chem. B* **2010**, 114, 10057. (c) Satpati, S. K.; Kumbhakar, M.; Nath, S.; Pal, H. *J. Photochem. Photobiol. A* **2008**, 200, 270. (d) Kumbhakar, M.; Singh, P. K.; Nath, S.; Bhasikuttan, A. C.; Pal, H. *J. Phys. Chem. B* **2008**, 112, 6646.
- (a) Adhikari, A.; Sahu, K.; Dey, S.; Ghosh, S.; Mandal, U.; Bhattacharyya, K. *J. Phys. Chem. B* **2007**, 111, 12809. (b) Jin, H.; Li, X.; Maroncelli, M. *J. Phys. Chem. B* **2007**, 111, 13473. (c) Bhattacharyya, K. *J. Phys. Chem. Lett.* **2010**, 1, 3254.
- (a) Jiang, W.; Wang, Y.; Yan, T.; Voth, G. A. *J. Phys. Chem. C* **2008**, 112, 1132. (b) Annappureddy, H. V. R.; Margulis, C. J. *J. Phys. Chem. B* **2009**, 113, 12005. (c) Bhargava, B. L.; Devane, R.; Klein, M. L.; Balasubramaniam, S. *Soft Matter* **2007**, 3, 1395. (d) Hu, Z.; Margulis, C. J. *Proc. Natl. Acad. Sci. U.S.A.* **2006**, 103, 833.
- (a) Triolo, A.; Russiana, O.; Bleif, H.-J.; Di Cola, E. *J. Phys. Chem. B* **2007**, 111, 4641. (b) Lopes, J. N. A. C.; Padua, A. A. H. *J. Phys. Chem. B* **2006**, 110, 3330. (c) Shiget, S.; Hamaguchi, H. *Chem. Phys. Lett.* **2006**, 427, 329.
- (a) Mandal, P. K.; Paul, A.; Samanta, A. *J. Photochem. Photobiol. A* **2006**, 182, 113. (b) Paul, A.; Mandal, P. K.; Samanta, A. *J. Phys. Chem. B* **2005**, 109, 9148.
- (a) Samanta, A. *J. Phys. Chem. Lett.* **2010**, 1, 1557. (b) Samanta, A. *J. Phys. Chem. B* **2006**, 110, 13704. (c) Santhosh, K.; Samanta, A. *J. Phys. Chem. B* **2010**, 114, 9195. (d) Santhosh, K.; Banerjee, S.; Rangaraj, N.; Samanta, A. *J. Phys. Chem. B* **2010**, 114, 1967. (e) Khara, D. C.; Paul, A.; Santosh, K.; Samanta, A. *J. Chem. Sci.* **2009**, 121, 309. (f) Paul, A.; Samanta, A. *J. Phys. Chem. B* **2007**, 111, 1957.
- (a) Mukherjee, P.; Crank, J. A.; Halder, M.; Armstrong, D. W.; Petrich, J. W. *J. Phys. Chem. A* **2006**, 110, 10725. (b) Chowdhury, P. K.; Halder, M.; Sanders, L.; Calhoun, T.; Anderson, J. L.; Armstrong, D. W.; Petrich, J. W. *J. Phys. Chem. B* **2004**, 108, 10245.
- (a) Dey, S.; Adhikari, A.; Das, D. K.; Sasmal, D. K.; Bhattacharyya, K. *J. Phys. Chem. B* **2009**, 113, 959. (b) Adhikari, A.; Dey, S.; Das, D. K.; Mandal, U.; Ghosh, S.; Bhattacharyya, K. *J. Phys. Chem. B* **2008**, 112, 6350. (c) Mondal, T.; Das, A. K.; Sasmal, D. K.; Bhattacharyya, K. *J. Phys. Chem. B* **2010**, 114, 13136.
- (a) Maroncelli, M.; Fleming, G. R. *J. Chem. Phys.* **1987**, 86, 6221. (b) Fee, R. S.; Maroncelli, M. *Chem. Phys.* **1994**, 183, 235.
- (a) Alexandridis, P.; Olsson, U.; Lindman, B. *Langmuir* **1998**, 14, 2627. (b) Ganguly, R.; Aswal, V. K.; Hassan, P. A.; Gopalakrishnan, I. K.; Yakhmi, J. V. *J. Phys. Chem. B* **2005**, 109, 5653.
- (a) Wanka, G.; Hoffmann, H.; Ulbricht, W. *Macromolecules* **1994**, 27, 4145. (b) Castner, E. W., Jr.; Kennedy, D.; Cave, R. J. *J. Phys. Chem. A* **2000**, 104, 2869.
- Rehm, D.; Weller, A. *Isr. J. Chem.* **1970**, 8, 259.



(21) (a) Ghosh, S.; Mandal, U.; Adhikari, A.; Bhattacharyya, K. *Chem. Asian J.* **2009**, *4*, 948. (b) Dey, S.; Mandal, U.; Sen Mojumdar, S.; Mandal, A. K.; Bhattacharyya, K. *J. Phys. Chem. B* **2010**, *114*, 15506. (c) Sasmal, D. K.; Mandal, A. K.; Mondal, T.; Bhattacharyya, K. Unpublished.

(22) Jones, G., II; Jackson, W. R.; Choi, C.-Y.; Bergmark, W. R. *J. Phys. Chem.* **1985**, *89*, 294.

(23) Tomida, D.; Kumagai, A.; Qiao, K.; Yokoyama, C. J. *Int. Thermophys.* **2006**, *27*, 39.

(24) (a) Quitevis, E. L.; Marcus, A. H.; Fayer, M. D. *J. Phys. Chem.* **1993**, *97*, 5762. (b) Wittouck, N. W.; Negri, R. M.; De Schryver, F. C. *J. Am. Chem. Soc.* **1994**, *116*, 10601. (c) Maiti, N. C.; Krishna, M. M. G.; Britto, P. J.; Periasamy, N. *J. Phys. Chem. B* **1997**, *101*, 11051. (d) Sen, S.; Sukul, D.; Dutta, P.; Bhattacharyya, K. *J. Phys. Chem. B* **2002**, *106*, 3763.

(25) (a) Sen, P.; Ghosh, S.; Sahu, K.; Mondal, S. K.; Roy, D.; Bhattacharyya, K. *J. Chem. Phys.* **2006**, *124*, 204905. (b) Mandal, D.; Sen, S.; Bhattacharyya, K.; Tahara, T. *Chem. Phys. Lett.* **2002**, *359*, 77.

(26) Kang, J. T.; Jarzeba, W.; Barbara, P. F.; Fonseca, T. *Chem. Phys.* **1990**, *149*, 81.